Available online at www.sciencedirect.com
SCIENCE DIRECT®
Biochemical Pharmacology 66 (2003) 415–424
Biochemical Pharmacology
www.elsevier.com/locate/biochempharm

# Chicken DT40 cells stably transfected with the rat $P2X_7$ receptor ion channel: a system suitable for the study of purine receptor-mediated cell death

Kate A. Hillman[a,b], Hitoshi Harada[c], Choong M. Chan[a,b], Andrea Townsend-Nicholson[a,1], Stephen E. Moss[d,2], Kengo Miyamoto[c], Yasunobu Suketa[c], Geoffrey Burnstock[a], Robert J. Unwin[a,b,d], Philip M. Dunn[a,*]

[a]*Autonomic Neuroscience Institute, Royal Free and University College Medical School, Rowland Hill Street, London NW3 2PF, UK*
[b]*Centre for Nephrology, Royal Free and University College Medical School, Rowland Hill Street, London NW3 2PF, UK*
[c]*Department of Environmental Biochemistry & Toxicology, School of Pharmaceutical Sciences, University of Shizuoka, 52-1 Yada, Shizuoka 422-8526, Japan*
[d]*Department of Physiology, Royal Free and University College Medical School, Rowland Hill Street, London NW3 2PF, UK*

Received 17 January 2003; accepted 4 April 2003

**Abstract**

We have generated and characterised a clone of chicken DT40 lymphocytes stably transfected with the rat $P2X_7$ receptor ($rP2X_7$). Successful transfection was confirmed by Western blotting. Under voltage clamp, $P2X_7$-expressing cells responded to ATP and dibenzoyl-ATP (Bz-ATP) (a more potent $P2X_7$ receptor agonist) with a rapidly activating and sustained inward current. The $EC_{50}$ values for these agonists were 305 and 15 μM, respectively. Bz-ATP evoked $Ca^{2+}$ and $Mn^{2+}$ influx into transfected cells as determined by Fura-2 spectrofluorimetry. Responses to Bz-ATP were inhibited by pre-treatment of cells with oxidised ATP. Treatment of cells with Bz-ATP for up to 24 hr produced time- and concentration-dependent cell death. This was associated with an increase in caspase-3-like activity, exposure of phosphatidylserine on the outside of cell membrane and DNA cleavage, indicating death by apoptosis. Pre-treatment with Z-VAD-fmk, a pan-caspase inhibitor, reduced the DNA fragmentation and phosphatidylserine externalisation, but did not affect overall rates of cell death at 24 hr, implicating caspase-independent mechanisms. The properties of $rP2X_7$ receptors expressed in DT40 cells are similar to those described for other expression systems. Because DT40 cells lack functionally detectable endogenous P2 receptors and are highly amenable to genetic manipulation, stably transfected DT40 cells provide a novel and potentially useful model system in which to investigate the intracellular signal transduction pathways associated with $P2X_7$ receptor stimulation, in particular those involved in induction of cell death.


*Keywords:* P2X receptor; ATP; Cell death; Apoptosis; Caspase; Lymphocyte

## 1. Introduction

Extracellular nucleotides play an important role in cell signalling with diverse effects, including modulation of cell growth, differentiation and induction of cell death by both necrosis and apoptosis [1,2]. The receptors for these molecules belong to two distinct families: P2Y G protein-coupled receptors and P2X ligand-gated ion channels. So far, molecular cloning has identified seven mammalian members of the P2Y group and seven P2X receptor subunits (see [3,4]). These latter subunits can combine to form either homo- or hetero-oligomeric receptors (of uncertain

* Corresponding author. Tel.: +44-207-830-2948; fax: +44-207-830-2949.
*E-mail address:* p.dunn@ucl.ac.uk (P.M. Dunn).
[1] Present address: Department of Biochemistry and Molecular Biology, University College London, Gower Street, London WC1E 6BT, UK.
[2] Present address: Division of Cell Biology, Institute of Ophthalmology, 11 Bath Street, London EC1V 9EL, UK.

*Abbreviations:* Bz-ATP, dibenzoyl-ATP; Z-VAD-fmk, *N*-benzyloxycarbonyl-Val-Ala-Asp(O-Me) fluoromethyl ketone; DMEM, Dulbecco's modified Eagle's medium; FCS, foetal calf serum; HBSS, Hanks' balanced salts solution; PBS, phosphate-buffered saline; NMG, *N*-methyl-D-glucamine; MTT, 3-(4,5-dimethyl-thiazol-2-yl)-2,5-diphenyltetrazolium bromide.

0006-2952/$ – see front matter © 2003 Elsevier Science Inc. All rights reserved.
doi:10.1016/S0006-2952(03)00286-7

stoichiometry) involving either three [5–7] or possibly four [8,9] subunits. The most recently identified member of the mammalian P2X family, the $P2X_7$ receptor, exhibits an interesting property. In addition to behaving as a rapidly activating non-selective cation channel, intense or prolonged activation of this receptor leads to the opening of a large non-selective pore allowing the passage of molecules of up to 900 Da in size [10,11]. This receptor shares 35–40% homology with other members of the P2X family with two transmembrane regions, a cysteine rich extracellular loop and intracellular N- and C-termini [12,13]. However, the C-terminal is over 100 amino acids longer than that of any other member of the family and may be essential for the unique features of the $P2X_7$ receptor, such as opening of the large pore [10] and mediation of cell blebbing *via* interaction with various membrane proteins [14,15]. This receptor appears to be identical to the pharmacologically identified P2Z receptor [16,17].

The mechanism by which activation of the $P2X_7$ receptor leads to the opening of a membrane-permeabilising pore is not well understood. The initial proposal describing the gradual increase in size of the cation channel to allow passage of larger molecules [18,19] is at variance with recent evidence that the receptor molecule itself may form some biochemical or structural link to a 'common pore,' which may also be opened by other membrane receptors, such as that for maititoxin [20,21], a toxin from the dinoflagellate *Gambierdiscus toxicus*.

Extracellular ATP can induce cell death in cells of the immune system, including thymocytes, T cells, macrophages and dendritic cells, through the activation of the P2Z/$P2X_7$ receptor. Cell death may occur through either necrosis [22] or apoptosis [23,24]. Furthermore, ATP can induce cell death in glomerular mesangial cells, which may have pathogenic implications for some forms of kidney disease [25,26]. However, functional studies of endogenous P2X receptors are complicated by the co-existence of multiple receptor subtypes (both P2X and P2Y) in the same native cell and a very limited array of subtype-specific pharmacological agonists or antagonists. This problem can be partially overcome by stable expression of recombinant receptors in a suitable 'null background' cell line.

DT40 is an avian leukosis virus-induced B cell line that continues diversification of its rearranged light chain immunoglobulin by gene conversion. Stable transfections of this cell line are unique in that they demonstrate an unexpectedly high ratio of targeted to random integration into the homologous gene loci, rendering them highly genetically tractable [27]. Wild-type DT40 cells show no rise in intracellular calcium concentration ($[Ca^{2+}]_i$) in response to various nucleotide agonists, indicating the lack of any endogenous purine receptors. In this study, we have generated DT40 cells stably transfected with the rat $P2X_7$ receptor. We have characterised the properties of these cells and demonstrated that activation of the $P2X_7$ receptor leads to cell death, which is associated with changes characteristic of apoptosis. This cell line could provide a useful model in which to study the regulatory and functional properties of the $P2X_7$ receptor, including investigation of the downstream signalling pathways leading to cell death.

## 2. Materials and methods

### 2.1. Drugs and reagents

Chicken serum, DMEM, FCS, glutamine and streptomycin were purchased from Gibco. Fura-2/AM and Pluronic F-127 were from Calbiochem. HBSS, EGTA, ATP, Bz-ATP and analogues, periodate oxidised ATP, and other chemicals were obtained from Sigma. Anti-$P2X_7$ antibody directed against the C-terminal 15 amino acids was purchased from Alomone Labs.

### 2.2. Cell culture and transfection

DT40 cells were routinely cultured at 40°, in DMEM supplemented with 10% FCS, penicillin, streptomycin, glutamine and 1% chicken serum and equilibrated with 5% $CO_2$. Cells were maintained in logarithmic growth and harvested for studies between $4 \times 10^5$ cells $mL^{-1}$ and $10 \times 10^5$ cells $mL^{-1}$. The rat $P2X_7$ cDNA construct (a generous gift of Dr. Gary Buell) in the mammalian expression vector pcDNA3 was linearised at the *Pvu*I site in the ampicillin resistance gene and the linearised DNA was re-suspended in sterile water at a concentration of 1 mg $mL^{-1}$ for use in transfection experiments. Transfection and selection of stable clones was carried out as described elsewhere [28].

### 2.3. Spectrofluorimetry

All experiments were performed on stirred cell suspensions at $10^6$ cells $mL^{-1}$ at 40° using an LS50 B fluorimeter (Perkin-Elmer). Cells were suspended in HBSS supplemented with HEPES, sodium bicarbonate and contained (in mM): 1.26 $CaCl_2$, 0.81 $MgSO_4$, 5.4 KCl, 0.44 $KH_2PO_4$, 136.9 NaCl, 0.34 $Na_2HPO_4$, 4.2 $NaHCO_3$, 5.5 D-glucose and 10 HEPES. EGTA (3 mM) was added for calcium-free experiments and agonists and antagonists added as indicated.

#### 2.3.1. Calcium fluorescence measurements

Measurements of intracellular free calcium concentration ($[Ca^{2+}]_i$) were made using the fluorescent indicator Fura-2. Cells (approximately $2.5 \times 10^6$) were loaded for 45 min in growth medium at 40° containing 1.25 μM Fura-2/AM and 0.0025% Pluronic F-127. Cells were washed three times and re-suspended at 4° in HBSS to a final density of $10^6$ cells $mL^{-1}$ and kept on ice for up to 1 hr. Cells were then pre-warmed to 40° in a water bath;

fluorescence of the stirred cell suspension was then measured by emission at 510 nm with excitation at 340 and 380 nm using an LS50 B fluorimeter (Perkin-Elmer). Removal of all residual extracellular calcium was achieved by addition of 3 mM EGTA at the beginning of fluorescence measurements.

*2.3.2. Manganese quench*

DT40 cells were loaded with Fura-2/AM as described above, washed three times and re-suspended in HBSS supplemented as above. Suspensions of cells at $10^6$ cells $mL^{-1}$ were pre-warmed to 40°; stirred samples were then excited at the dye's isosbestic wavelength of 360 nm and emission monitored at 510 nm. Antagonists and agonists were added from stock solutions to the desired concentrations at 50 and 150 s after the addition of 100 μM manganese ($Mn^{2+}$), respectively.

*2.3.3. Ethidium bromide influx*

Cells were washed three times in HBSS, warmed to 40° and placed in a cuvette at $10^6$ cells $mL^{-1}$. Twenty-five μM ethidium bromide was added and fluorescence recorded as a function of time: cells were excited at 302 nm and emission monitored at 560 nm. Fluorescence values were corrected for background fluorescence, a small concentration-dependent quenching of fluorescence by Bz-ATP and expressed as a percentage of the maximum value obtained following complete permeabilisation of the cells with 10 μM digitonin.

*2.3.4. Western blotting*

$10^7$ cells were washed twice in PBS and re-suspended in 100 μL SDS–PAGE buffer in the presence of protease inhibitors (phenylmethylsulfonyl fluoride, PMSF) 0.5 mM and 1 μM of each of the small peptidase inhibitors, chymostatin, leupeptin and pepstatin) on ice. After DNA shearing using an 18G needle, extracts were boiled for 15 min and separated on a 10% polyacrylamide gel and transferred to nitrocellulose membrane. Nitrocellulose membranes were incubated with primary antibody followed by alkaline phosphatase-conjugated swine anti-rabbit immunoglobulins and developed using Western Blue.

*2.3.5. Electrophysiology*

A small volume (50–200 μL) of cell suspension (approximately $10^5$ cells $mL^{-1}$) was plated out in a 35 mm plastic culture dish (Falcon) containing 2 mL extracellular solution at 37°. The dish was then left to cool to room temperature (19–22°). Using this procedure, the majority of cells adhered adequately to the culture dish.

The culture dish was placed on the stage of an inverted microscope (Diaphot, Nikon) and cells visualised under phase contrast at 600× magnification. For most experiments, the culture dish was perfused at a rate of 0.5 mL $min^{-1}$ with an extracellular-like solution containing (mM): NaCl, 154, KCl 4.7, HEPES, 10, D-glucose, 5.6, $CaCl_2$ 2.5, $MgCl_2$ 1.2, adjusted to pH 7.4 with NaOH, while low divalent cation solution (containing 0 mM $MgCl_2$ and 0.5 mM $CaCl_2$) was applied locally to cells using a microperfusion device [29]. For experiments carried out at 30°, the culture dish was perfused at 5 mL $min^{-1}$ with pre-warmed low divalent cation extracellular solution, and drugs were applied in the perfusing solution. NMG-containing solution was made by equimolar substitution of $Na^+$ by NMG. For experiments to determine the relative ionic permeabilities, a simplified solution containing no $K^+$ or divalent cations was used.

Recordings were carried out using the whole cell patch-clamp technique [30]. Patch electrodes were fabricated from thin wall borosilicate glass capillaries (Clark Electromedical, GC 150TF) and had a resistance of 4–6 MΩ when filled with an intracellular-like solution containing (mM): citric acid 56, $MgCl_2$ 3, CsCl 20, HEPES, 40, EGTA 0.1, tetraethyl ammonium chloride 10, adjusted to pH 7.2 with CsOH. Membrane currents were recorded using an Axopatch 200B amplifier (Axon Instruments), displayed on a chart recorder (Gould TA240) and stored on digital audiotape using a DTR-1204 (Biologic, Claix) recorder for subsequent off-line analysis. Ramp current voltage relationships were recorded on a personal computer, using pClamp software and a Digidata 1200 interface (Axon Instruments).

*2.3.6. Assay of cell viability*

Assay of cell viability was carried out using the Cell Proliferation Kit I (MTT), according to the manufacturer's instructions. One day before experiments, cells were plated in 96-well culture plates at a density of $1 \times 10^5$ per well. Antagonists of $P2X_7$ and caspases, oxidised ATP and Z-VAD-fmk, respectively, were applied for 1 hr prior to agonists. After treatments with ATP or Bz-ATP, cells were incubated in MTT solution for 4 hr at 37°. Absorbance was measured with a microplate reader and test filter of 540 nm and a reference filter of 620 nm.

*2.3.7. Assay for caspase-3-like protease activity*

Caspase-3-like protease activity was measured using the EnzChek Caspase-3 Assay Kit (Molecular Probes). After incubation with appropriate agonists and antagonists, cells were collected and washed three times with PBS, and re-suspended in hypotonic cell lysis buffer (25 mM HEPES [pH 7.5], 5 mM $MgCl_2$, 5 mM EDTA, 5 mM dithiothreitol, 2 mM PMSF, 10 μg $mL^{-1}$ aprotinin, 10 μg $mL^{-1}$ leupeptin). The cells were incubated on ice for 20 min and then homogenised. Lysates were centrifuged at 45,000 *g* for 60 min at 4° and supernatants were collected. Aliquots of lysate containing 2.5 μg protein were incubated with *N*-benzyloxycarbonyl-Asp-Glu-Val-Asp-7-amino-4-methyl-coumarin (Z-DEVD-AMC; 5 μM) at 37° and the release of 7-amino-4-methyl-coumarin (AMC) was monitored by a spectrofluorometer (Hitachi F-2000) using an excitation wavelength of 380 nm and an emission wavelength of 460 nm.

*2.3.8. Detection of exposure of phosphatidylserine on the outside of the cell membrane*

To detect the early membrane changes of apoptosis, the annexin-V-FLUOS staining kit was used for flow cytometric detection of phosphatidylserine externalisation on the outside of the cell membrane. Annexin-V has a high and selective affinity for phosphatidylserine [31]. In brief, cells were suspended in DMEM-F-12/10% FCS/0.1% chick serum, and treated with drugs for 6 hr. The cells were washed with PBS and incubated for 15 min at room temperature with 0.25 μg $mL^{-1}$ of FITC-annexin-V and 10 μM propidium iodide. At least 10,000 cells were analysed and apoptosis (FITC-positive and propidium iodide negative-cells) was assessed by flow cytometry (COULTER EPICS-XL).

*2.3.9. DNA ladder detection assay*

After treatment with indicated reagents for 6 hr, cells were washed with PBS, lysed with 150 μL of lysis buffer (10 mM Tris–HCl, pH 7.4, 10 mM EDTA, 0.5% Triton X-100) for 20 min on ice and precipitated with 2.5% polyethylene glycol and 1 M NaCl at 4°. After centrifugation at 10,000 *g* for 10 min, supernatants were incubated in RNase A (400 μg $mL^{-1}$) for 1 hr, subsequently treated with proteinase K (400 μg $mL^{-1}$) for 1 hr, and then precipitated with equal volumes of isopropanol at −20° overnight. After washing with 70% ethanol, each pellet was dissolved in 20 μL of TE buffer and electrophoresed on a 2% agarose gel containing ethidium bromide. Ladder formation of oligonucleosomal DNA was visualised under ultraviolet light.

*2.4. Data analysis*

All data are expressed as mean ± SEM. Concentration–response curves were fitted with the Hill equation, $Y = A/[1 + (K/X)^n]$, using a commercial graphics and data analysis software package (Origin v4, Microcal). Traces were acquired using Fetchex (pClamp software, Axon Instruments) and plotted using Origin. Statistical analysis was performed using Instat version 2.0 statistical package (GraphPad Software). $P < 0.01$ was taken as statistically significant.

## 3. Results

Following transfection, a number of clones were isolated and characterised functionally and biochemically for the expression of the $P2X_7$ receptor. Six clones were identified on the basis of functional responses to Bz-ATP, but all the data presented have been obtained from one representative clone.

*3.1. Molecular characterisation*

To confirm the successful transfection of the $rP2X_7$ construct into DT40 cells, we detected receptor protein by Western blotting. In transfected cells, the anti-$P2X_7$ antibody identified a protein band with a molecular weight of approximately 70 kDa. No band was detected in protein extracts from wild-type or vector-only transfected controls (Fig. 1A).

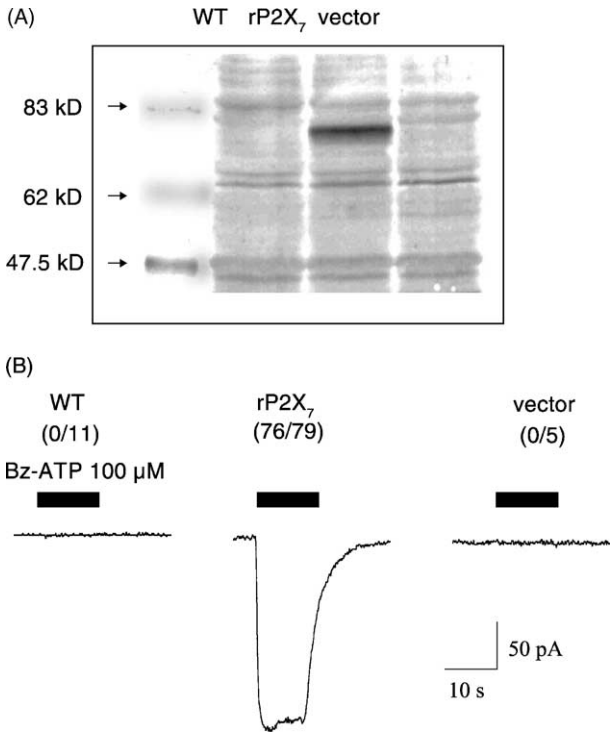


Fig. 1. Expression of $rP2X_7$ receptors in transfected DT40 cells. (A) Western blot analysis demonstrates the presence of $rP2X_7$ receptor protein (MW ~70 kDa) in DT40 cells after cDNA transfection. However, protein was absent in wild-type (WT) and vector-only transfected cells. (B) Patch-clamp recording from wild-type, vector-only transfected and $rP2X_7$ transfected DT40 cells. While 76/79 transfected cells responded to 100 μM Bz-ATP with a rapidly activating and sustained inward current, no response was observed in wild-type or mock transfected cells.

*3.2. Functional characterisation*

The properties of transfected cells were assessed at both the single cell level by whole cell patch-clamp technique and as an average of activities of cell populations by fluorimetry. Cells from the $P2X_7$ transfected clone voltage-clamped at −60 mV responded to the application of Bz-ATP with a rapidly activating inward current. The response was maintained throughout the drug application and the current returned to baseline on removal of the agonist (Fig. 1B). Such responses were seen in 96% (76/79) of cells tested. The mean amplitude of the response to 100 μM Bz-ATP was 217 ± 40 pA (N = 21) from cells that had a mean membrane capacitance of 4.2 ± 0.2 pF. ATP also evoked similar responses, although this agonist was considerably less potent (see below). In contrast, Bz-ATP failed to evoke any response in 11 wild-type cells or 5 cells from a mock (vector-only) transfected clone.

### 3.3. Concentration-dependence

Fig. 2A demonstrates the concentration-dependence of the activation of the $P2X_7$ receptor using electrophysiological recordings. The sustained nature of the $P2X_7$ response allowed cumulative concentration–effect curves to be obtained for ATP and Bz-ATP (Fig. 2B). Fitting the Hill equation to the pooled data gave $EC_{50}$ values of

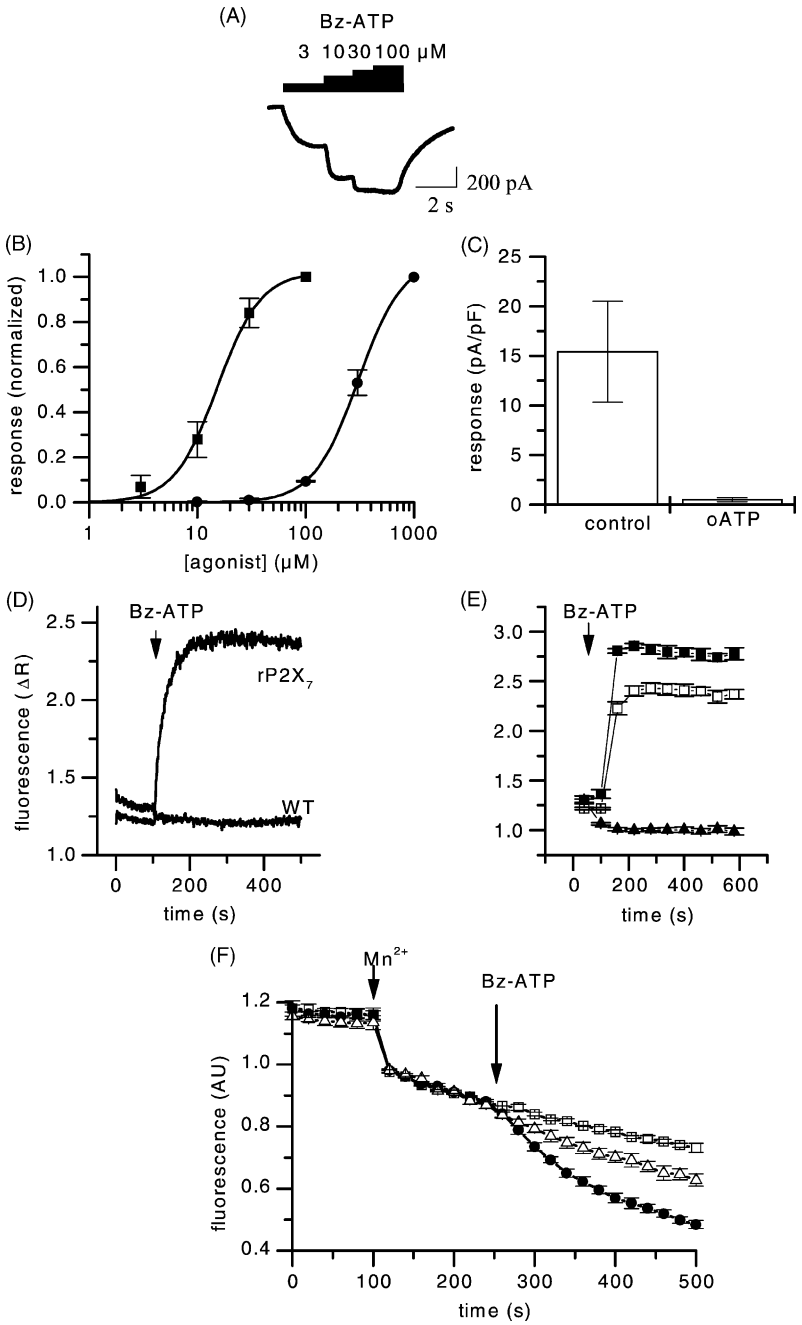


Fig. 2. Functional characterisation of transfected DT40 cells. (A) The effect of increasing agonist concentration on the inward current recorded from a $rP2X_7$ transfected cell voltage clamped at −60 mV. (B) Concentration–response curves for the activation of inward currents in transfected DT40 cells under voltage clamp at room temperature. Points represent mean ± SEM from 10 cells (Bz-ATP; ■) and 5 cells (ATP; ●) normalised with respect to the highest concentration of agonist used. The curves show the least squares fit of the Hill equation to the data, which yielded $EC_{50}$ values of 15 and 305 µM for Bz-ATP and ATP, respectively. (C) Histogram comparing the response of control cells to 100 µM Bz-ATP with cells that had been pre-incubated with 100 µM oxidised ATP (oATP) for 2 hr at 37°. Columns represent the mean ± SEM current density for 10 cells. (D) Fura-2 measurement of intracellular $[Ca^{2+}]_i$ concentration in DT40 cells. Bz-ATP (50 µM) induced an increase in $[Ca^{2+}]_i$ in transfected but not wild-type DT40 cells. (E) Comparison of the effect of 50 µM (□) and 100 µM (■) Bz-ATP on $[Ca^{2+}]_i$ with the response to 100 µM Bz-ATP after removal of extracellular $Ca^{2+}$ by the addition of 3 mM EGTA (▲). Experiments were carried out at 40°. Points represent mean ± SEM from three experiments. (F) The increase in divalent cation permeability in transfected DT40 cells in response to Bz-ATP (100 µM) determined using the manganese quench technique. Addition of $Mn^{2+}$ produced a biphasic decline in fluorescence (□). Subsequent addition of Bz-ATP produced a further decline in fluorescence (●). In cells pre-incubated for 2 hr with 100 µM oxidised ATP (△) there was an approximately 50% reduction in the response to Bz-ATP. Points represent the mean ± SEM from three experiments.

15.3 ± 1.2 μM and 305.5 ± 2.4 μM with Hill coefficients of 2.2 ± 0.4 and 2.1 ± 0.1 for Bz-ATP (data from 10 cells) and ATP (data from 5 cells), respectively.

Oxidised ATP is a slowly acting antagonist at the $P2X_7$ receptor [32]. In patch-clamp experiments, a 2-hr incubation at 37° with 100 μM oxidised ATP almost completely abolished the inward current evoked by Bz-ATP (Fig. 2C).

### 3.4. Calcium influx in cell suspensions

Addition of Bz-ATP (50 μM) to a suspension of $P2X_7$-transfected cells produced a rapid and sustained increase in intracellular [$Ca^{2+}$] determined by the change in Fura-2 fluorescence (Fig. 2D). No such change was observed in wild-type or mock transfected cells (not shown). A slightly greater influx of $Ca^{2+}$ was obtained by increasing the Bz-ATP concentration to 100 μM. However, when the experiment was repeated in the absence of extracellular $Ca^{2+}$ (and in the presence of 3 mM EGTA), no increase in intracellular [$Ca^{2+}$] was observed, confirming that the response was due to $Ca^{2+}$ influx across the cell membrane and not release from intracellular stores (Fig. 2E).

We investigated the effect of oxidised ATP on divalent cation permeability using the manganese quench technique. Application of the agonist Bz-ATP to a suspension of $P2X_7$-transfected cells in the presence of $Mn^{2+}$ produced a dramatic reduction in Fura-2 fluorescence (Fig. 2F). Pre-incubation of transfected cells with oxidised ATP for 1 hr produced a concentration-dependent reduction in the Bz-ATP stimulated $Mn^{2+}$ influx. At 100 μM oxidised ATP, the $Mn^{2+}$ influx was significantly attenuated (Fig. 2F), while at 300 μM, it was completely abolished (data not shown).

### 3.5. Ion permeability

Prolonged activation of the $P2X_7$ receptor in low divalent cation-containing solution, or at near physiological temperature has been reported to lead to the opening of a cytolytic pore allowing the passage of molecules with molecular weight of up to approximately 900 Da, which can be detected electrophysiologically by a shift in the reversal potential in $NMG^+$-containing solution [19]. Therefore, we determined the relative permeability of the channel to NMG when expressed in DT40 cells. For these experiments, a simplified extracellular solution containing only HEPES, 10 mM, glucose, 10 mM and XCl, 164 mM (where X = either $Na^+$ or $NMG^+$) was used. Under these conditions, the reversal potential shifted from 2.5 ± 1.6 mV in $Na^+$ solution to −62.6 ± 3.0 mV in $NMG^+$ (N = 4), yielding a value of $P_{NMG}/P_{Na}$ of 0.06. Interestingly, when the $NMG^+$ solution also contained 0.5 mM $Ca^{2+}$, the reversal potential was 12 mV more positive, indicating that this channel has a high permeability to $Ca^{2+}$. These experiments were conducted at room temperature, and no time-dependent change in the reversal

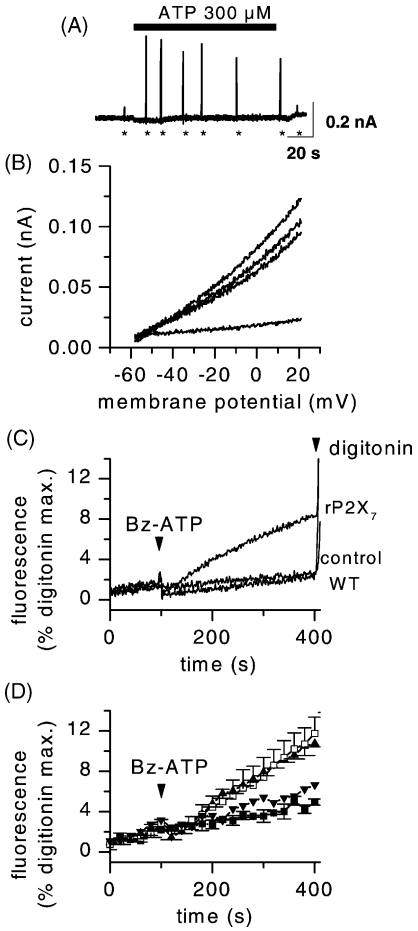


Fig. 3. Permeability of $P2X_7$ transfected DT40 cells to large cations. (A) Response of a voltage-clamped DT40 cell to application of ATP (300 μM) for 2 min at 30° in NMG-containing extracellular solution. Voltage ramps were injected at the times indicated by the asterisks, to determine, the current–voltage relationship. Four of these are shown in (B). Although there was some reduction in the amplitude of the response during the 2 min agonist application, the reversal potential remained constant at −55 mV. Similar results were observed in a further three cells. (C) Increasing ethidium bromide fluorescence in response to Bz-ATP (100 μM) in transfected DT40 cells. In wild-type cells, there was a small increase in fluorescence comparable to that seen in unstimulated cells. (D) Comparison of ethidium uptake stimulated by 100 μM (□) and 200 μM (▲) Bz-ATP with that of unstimulated cells (■) and that produced by 100 μM Bz-ATP in cells pre-treated with 100 μM oxidised ATP (▼).

potential was observed (data not shown). We therefore determined the reversal potential in $NMG^+$ solution during prolonged activation of the receptor at 30°. Fig. 3A and B illustrate one such experiment. Application of 300 μM ATP for 2 min evoked a very small inward current with a reversal potential close to −60 mV. No initial outward current, slow increase in inward current or changes in reversal potential were observed during the agonist application. Similar results were obtained in a further three cells.

Further assessment of the pore-forming properties of the $P2X_7$ receptor was undertaken using fluorimetry. Incubation of cells at 40° for 5 min in the presence of ethidium bromide produced a small basal increase in fluorescence in

both wild-type and transfected DT40 cells. In the presence of 100 or 200 μM Bz-ATP, a small agonist-dependent increase in fluorescence was observed, which at 5 min was less than 10% of maximal fluorescence produced by the permeabilisation of the cells with digitonin (Fig. 3C). The small baseline increase in ethidium fluorescence was comparable in wild-type and transfected cells. Although the Bz-ATP-induced ethidium entry is small, this effect appears to be due to the presence of the $P2X_7$ receptor, since it was not observed in wild-type cells and could be partially blocked by pre-incubation of the cells with 100 μM oxidised ATP (Fig. 3D).

### 3.6. $P2X_7$ agonist-induced cell death

Prolonged incubation of transfected DT40 cells with ATP or Bz-ATP produced a dramatic reduction in cell viability. Fig. 4A shows the concentration-dependence of this effect when cells were incubated with ATP or Bz-ATP, for 24 hr. No comparable changes in viability were observed in wild-type or mock-transfected cells (data not shown). Bz-ATP was approximately ten times more potent than ATP. Treatment with 100 μM Bz-ATP for increasing periods of time produces progressive reduction in cell viability (Fig. 4B), with over 80% of cells dying 18 hr after a 6 hr incubation with the agonist. This reduction in cell viability by Bz-ATP was completely inhibited by 300 μM oxidised ATP or by addition of 5 mM magnesium chloride to the culture medium (Fig. 4C). Both treatments are known to block $P2X_7$ activation. These results directly demonstrate that activation of $P2X_7$ receptor-induced cell death.

### 3.7. Activation of a caspase-3(-like) protease by $P2X_7$ agonists

To analyse further the biological events associated with $P2X_7$-induced cell death, we investigated the activation of caspase-3(-like) protease activity. Fig. 5A shows the activity of caspase-3(-like) protease in cells cultured with 200 μM Bz-ATP for increasing periods of time. We also observed a similar activation of caspase-3(-like) protease by treatment with ATP (data not shown). In keeping with the involvement of $P2X_7$ receptors, this agonist was considerably less potent than Bz-ATP. Following prolonged (24 hr) treatment with 200 μM Bz-ATP, or 12 hr treatment with 300 μM Bz-ATP, the protease activity was decreased. The reason for this is at present unclear, but it may indicate more rapid and complete cell death, and thus loss of caspase-3-like activity. To confirm that caspase-3(-like) protease was activated by stimulation of $P2X_7$ receptors, the effect of oxidised ATP, an irreversible inhibitor of the $P2X_7$ receptor, was also examined. As shown in Fig. 5B, when the cells were pre-treated with 200 μM oxidised ATP for 3 hr prior to challenge with 200 μM Bz-ATP, protease activation was reduced by 73%.

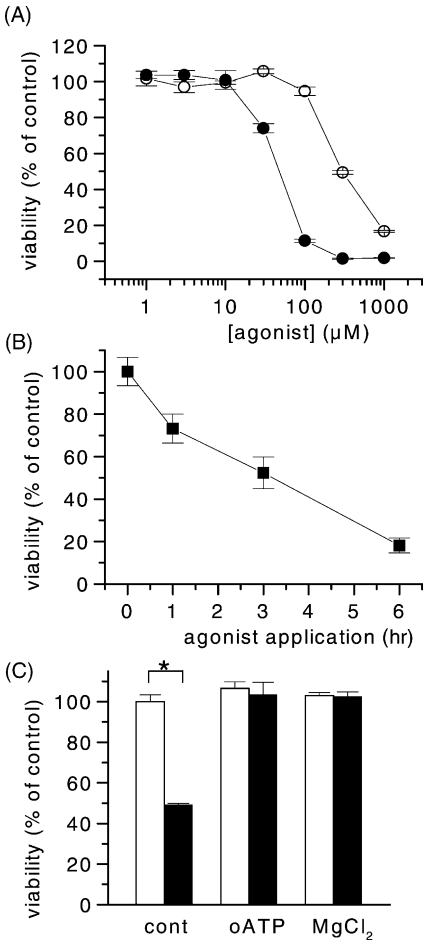


Fig. 4. Effect of $P2X_7$ receptor activation on cell viability in transfected DT40 cells. (A) Concentration–response curve for the decrease in cell viability produced by ATP (○) and Bz-ATP (●) measured after 24 hr incubation with the agonist. Cell viability was determined by succinate-tetrazolium reductase activity. (B) Effect of the duration of agonist application on cell viability. Transfected cells were incubated with 100 μM Bz-ATP for indicated times, then washed with Bz-ATP-free medium and cell viability measured 24 hr after Bz-ATP exposure. (C) Effects of $P2X_7$ antagonist oxidised ATP (oATP) and $MgCl_2$ on Bz-ATP-induced reduction in cell viability. Cells were pre-treated with 300 μM oxidised ATP or 5 mM $MgCl_2$ for 1 hr, exposed to 100 μM Bz-ATP for 3 hr, and then washed with Bz-ATP-free medium. Cell viability was measured 24 hr after Bz-ATP treatment (■) and in time matched untreated cells (□). Bars represent the mean ± SD from three experiments. An asterisk (*) significantly different $P < 0.01$.

### 3.8. The role of apoptosis in $P2X_7$ receptor-induced cell death

The generation of caspase-3-like activity by $P2X_7$ receptor activation would be consistent with cell death occurring by apoptosis. To confirm this, we looked at two other markers of apoptosis, namely DNA laddering, and phosphatidylserine externalisation [33,34], and investigated the effects of the pan-caspase inhibitor Z-VAD-fmk.

Treatment of cells for 6 hr with 100 μM Bz-ATP resulted in a dramatic increase in the number of cells with phosphatidylserine on the outside of the cell membrane, which was greatly reduced by incubating the cells with 60 μM

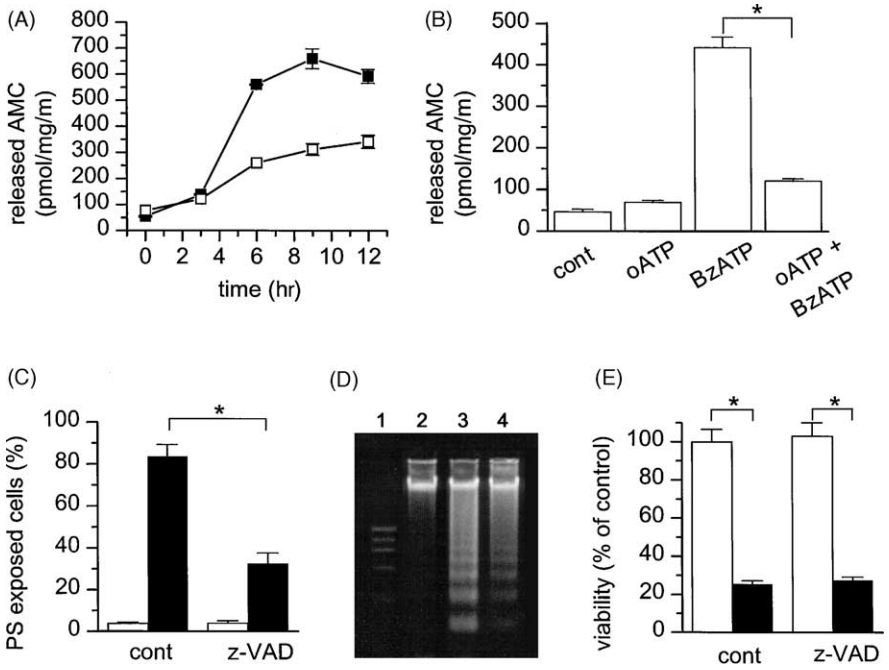


Fig. 5. Involvement of caspase activation in $P2X_7$-mediated cell death. (A) Time-dependence of the stimulation of caspase-3-(like) activity by Bz-ATP in transfected DT40 cells. Cells were treated with Bz-ATP 100 μM (□) or 200 μM (■) for the indicated times. (B) Inhibition of Bz-ATP-stimulated caspase-3-(like) activity by oxidised ATP (oATP). Cells were pre-treated with oATP 200 μM for 3 hr, washed with oATP-free medium and then treated with or without Bz-ATP for 12 hr. The cells were then lysed and caspase-3-(like) activity determined by measuring the release of AMC. Columns represent the mean ± SEM from three experiments. (C) Inhibition of Bz-ATP-induced exposure of phosphatidylserine on the outside of cell membrane by Z-VAD-fmk. Cells were pre-treated with or without 60 μM Z-VAD-fmk for 1 hr and then treated with (■) or without (□) Bz-ATP 100 μM for 6 hr. Phosphatidylserine on the outside of cell membrane was detected using the annexin-V-FLUOS staining kit. (D) Bz-ATP-induced DNA fragmentation is inhibited by Z-VAD-fmk. Cells were pre-treated with 60 μM Z-VAD-fmk for 1 hr and then treated with Bz-ATP 100 μM for 6 hr. Oligonucleosomal DNA was extracted and electrophoresed on agarose gel containing ethidium bromide. Fragmented DNA was visualised under ultraviolet light. Lane 1: DNA size marker (X174 DNA/*Hae*III digest), lane 2: untreated cells, lane 3: Bz-ATP, lane 4: Z-VAD-fmk and Bz-ATP. (E) Effect of Z-VAD-fmk on Bz-ATP-induced reduction in cell viability. Cells were pre-treated with Z-VAD-fmk 100 μM for 1 hr and then treated with Bz-ATP 100 μM for 3 hr. After 3 hr cells were washed with Z-VAD-fmk-free and Bz-ATP-free medium, and cell viability assessed 24 hr after agonist application, using MTT assay. An asterisk (∗) significantly different $P < 0.01$.

Z-VAD-fmk (Fig. 5C). Treatment of cells for 6 hr with 100 μM Bz-ATP also gave rise to the formation of typical ladders of oligonucleosomal fragments of extracted DNA (Fig. 5D). This was also attenuated by treatment with 60 μM Z-VAD-fmk. These results support the view that the cytotoxicity of $P2X_7$ agonists on $rP2X_7$ transfected DT40 cells is *via* the induction of apoptosis. Finally, we examined the effect of the pan-caspase inhibitor on Bz-ATP-induced cell death. Surprisingly, the overall reduction in cell viability induced by 3 hr treatment with 100 μM Bz-ATP was not altered by pre-treatment with 100 μM Z-VAD-fmk for 1 hr (Fig. 5E).

## 4. Discussion

The $P2X_7$ receptor is expressed in many different cell types, in which its activation can stimulate proliferation [35], or cause cell death by necrosis or apoptosis [22,25,26,36–38]. However, the downstream signalling pathways involved in these different effects are still poorly understood. The function of the $P2X_7$ receptor has been studied using a range of endogenously-expressing cell lines, such as immune cells, macrophages, microglial cells and monocytes, and in a range of transfected cell lines, including HEK-293 [19], human astrocytoma cell lines [39] and Xenopus oocytes [40]. Unfortunately, in the endogenously-expressing cell types, there is frequently native co-expression of other purine receptors (both P1 and P2), which along with the current lack of specific antagonists or agonists for these receptors, impedes study of individual receptor molecules and their downstream signal transduction pathways.

We have chosen to express the rat $P2X_7$ receptor onto a 'null' background using the DT40 avian lymphocyte, which lacks any endogenous purinoceptors. The other major advantage of the DT40 cell line is its unique genetic tractability, demonstrating high ratios of targeted to random gene integration into the homologous gene loci when compared with mammalian cell lines, which is a result of continued diversification of its rearranged light chain immunoglobulin by gene conversion [27]. This has led to the increasing use of the DT40 cell in studies of a wide range of higher organism cellular functions, including control of calcium signalling [28], oxidative stress signalling and apoptotic pathways [41,42]. Knockout of candidate molecules, and taking advantage of this tractability, should facilitate investigation of the signal transduction

pathways linked to $P2X_7$ receptor activation and induction of cell death or other downstream events, and also help in the identification of regulatory mechanisms.

The properties of the $rP2X_7$ expressed in DT40 cells were similar to those observed in other expression systems [10,39]. Thus, Bz-ATP was a more potent agonist than ATP, and the receptor was blocked by prolonged incubation with oxidised ATP. Activation of the $rP2X_7$ receptor in DT40 cells opened a non-selective cation conductance, which had a significant permeability to $Ca^{2+}$, as determined by both intracellular $[Ca^{2+}]_i$ measurement using Fura-2, and by the shift in reversal potential observed on removal of extracellular $Ca^{2+}$. Although the relative permeability of the channel to NMG ($P_{NMG}/P_{Na} = 0.03$) was very similar to that reported by Virginio *et al*. [19], we did not observe a time-dependent increase in NMG permeability, which would have indicated the formation of a cytolytic pore; however, we were able to demonstrate a small amount of ethidium uptake following stimulation with Bz-ATP.

The formation of a large cytolytic pore following $P2X_7$ receptor activation has been observed in a wide variety of cell types, suggesting that opening of the pore is a further conformational change of the $P2X_7$ receptor [18,19]. More recently, it has been suggested that both $P2X_7$ receptors and the dinoflagellate toxin maitotoxin activate a common pore, and that the efficiency of the coupling between receptor and pore varies between cell types. If true, then our results indicate that the coupling in DT40 cells, like that in BW5147.3 lymphoma cells, is weak [20,21].

Following exposure to the $P2X_7$ receptor agonist, DT40 cells expressing $rP2X_7$ receptors were killed. This was accompanied by exposure of phosphatidylserine on the outside of cell membrane and DNA laddering, suggesting that death was occurring by apoptosis. At present, it is not clear how cell death, which occurred over many hours, is related to the almost immediate changes in membrane ion permeability and elevation in $[Ca^{2+}]_i$. One possibility is that $P2X_7$-mediated cell death is dependent on the formation of the cytolytic pore. In which case, the poor coupling we observed between receptor activation and pore formation in DT40 cells might account for the long delay between receptor activation and cell death. However, in hepatocytes, ATP-induced cell death is dependent on a rise in intracellular calcium, leading to accumulation of $Ca^{2+}$ in mitochondria, and loss of mitochondrial membrane potential [44]. This may lead to cytochrome *c* release and the activation of a cascade of cysteine proteases (caspases) which are known to be involved in programmed cell death [24,43]. Consistent with this, elevation of intracellular $Ca^{2+}$ produces mitochondrial swelling in DT40 cells [45], and we demonstrated that activation of $rP2X_7$ receptors in DT40 cells leads to an increase in caspase-3-like activity. However, blockade of the caspase enzyme activation, despite reducing DNA laddering and phosphatidylserine externalisation, did not affect the overall reduction in cell viability induced by $P2X_7$ agonists in this transfected cell line. Further studies will be necessary to elucidate the exact role of intracellular $Ca^{2+}$, mitochondrial cytochrome *c* release and the activation of caspases in $P2X_7$ receptor-triggered cell death of DT40 cells.

In conclusion, we have generated a novel cell line of DT40 avian B lymphocytes stably transfected with the rat $P2X_7$ receptor and we have characterised its properties in detail using a variety of methods. The properties of the expressed rat $P2X_7$ receptor were broadly similar to those described in other expression systems, but we observed only weak coupling to the formation of a cytolytic pore. These cells underwent reproducible reduction in cell viability following exposure to $P2X_7$ receptor agonists, which was associated with, the stimulation of caspase-3-like protease activity. Since these cells are highly genetically tractable [27], they should prove a very useful model for elucidating the physiological role of the $P2X_7$ receptor, its downstream signalling pathways linked to cell death by apoptosis and aid the development of highly selective agonists and antagonists.

## Acknowledgments

This work was supported in part by a grant-in-aid for encouragement of young scientists from the Ministry of Education, Science and Culture, Japan (H. Harada), the Medical Research Council, UK (C.M. Chan, R.J. Unwin, G. Burnstock), the Special Trustees of the Middlesex Hospital and the St. Peter's Trust, UK (C.M. Chan), Roche Bioscience, Palo Alto, CA (P.M. Dunn) and the National Kidney Research Fund, UK (K.A. Hillman). We are grateful to Chrystalla Orphanides for editorial assistance.

## References

[1] Zheng LM, Zychlinsky A, Liu CC, Ojcius DM, Young JDE. Extracellular ATP as a trigger for apoptosis or programmed cell death. J Cell Biol 1991;112:279–88.
[2] Chow SC, Kass GE, Orrenius S. Purines and their roles in apoptosis. Neuropharmacology 1997;36:1149–56.
[3] Abbracchio MP, Burnstock G. Purinoceptors: are there families of P2X and $P_{2Y}$ purinoceptors? Pharmacol Ther 1994;64:445–75.
[4] Zhang FL, Luo L, Gustafson E, Palmer K, Qiao X, Fan X, Yang S, Laz TM, Bayne M, Monsma Jr F. P2Y(13): identification and characterization of a novel Galphai-coupled ADP receptor from human and mouse. J Pharmacol Exp Ther 2002;301:705–13.
[5] Nicke A, Baumert HG, Rettinger J, Eichele A, Lambrecht G, Mutschler E, Schmalzing G. $P2X_1$ and $P2X_3$ receptors form stable trimers: a novel structural motif of ligand-gated ion channels. EMBO J 1998;17:3016–28.
[6] Ding S, Sachs F. Single channel properties of $P2X_2$ purinoceptors. J Gen Physiol 1999;113:695–720.
[7] Stoop R, Thomas S, Rassendren F, Kawashima E, Buell G, Surprenant A, North RA. Contribution of individual subunits to the multimeric $P2X_2$ receptor: estimates based on methanethiosulfonate block at T336C. Mol Pharmacol 1999;56:973–81.
[8] Kim M, Yoo OJ, Choe S. Molecular assembly of the extracellular domain of $P2X_2$, an ATP-gated ion channel. Biochem Biophys Res Commun 1997;240:618–22.

[9] Ding S, Sachs F. Inactivation of $P2X_2$ purinoceptors by divalent cations. J Physiol (London) 2000;522:199–214.
[10] Surprenant A, Rassendren F, Kawashima E, North RA, Buell G. The cytolytic P2Z receptor for extracellular ATP identified as a P2X receptor ($P2X_7$). Science 1996;272:735–8.
[11] Rassendren F, Buell GN, Virginio C, Collo G, North RA, Surprenant A. The permeabilizing ATP receptor, $P2X_7$. Cloning and expression of a human cDNA. J Biol Chem 1997;272:5482–6.
[12] Valera S, Hussy N, Evans RJ, Adani N, North RA, Surprenant A, Buell G. A new class of ligand-gated ion channel defined by P2X receptor for extracellular ATP. Nature 1994;371:516–9.
[13] Hansen MA, Barden JA, Balcar VJ, Keay KA, Bennett MR. Structural motif and characteristics of the extracellular domain of P2X receptors. Biochem Biophys Res Commun 1997;236:670–5.
[14] Kim M, Jiang LH, Wilson HL, North RA, Surprenant A. Proteomic and functional evidence for a $P2X_7$ receptor signalling complex. EMBO J 2001;20:6347–58.
[15] Wilson HL, Wilson SA, Surprenant A, North RA. Epithelial membrane proteins induce membrane blebbing and interact with the $P2X_7$ receptor C-terminus. J Biol Chem 2002;277:34017–23.
[16] Nuttle LC, El Moatassim C, Dubyak GR. Expression of the pore-forming P2Z purinoceptor in Xenopus oocytes injected with poly(A)$^+$ RNA from murine macrophages. Mol Pharmacol 1993;44:93–101.
[17] Wiley JS, Gargett CE, Zhang W, Snook MB, Jamieson GP. Partial agonists and antagonists reveal a second permeability state of human lymphocyte P2Z/$P2X_7$ channel. Am J Physiol 1998;275:C1224–31.
[18] Chessell IP, Michel AD, Humphrey PP. Properties of the pore-forming $P2X_7$ purinoceptor in mouse NTW8 microglial cells. Br J Pharmacol 1997;121:1429–37.
[19] Virginio C, MacKenzie A, North RA, Surprenant A. Kinetics of cell lysis, dye uptake and permeability changes in cells expressing the rat $P2X_7$ receptor. J Physiol (London) 1999;519:335–46.
[20] Schilling WP, Sinkins WG, Estacion M. Maitotoxin activates a non-selective cation channel and a P2Z/$P2X_7$-like cytolytic pore in human skin fibroblasts. Am J Physiol 1999;277:C755–65.
[21] Schilling WP, Wasylyna T, Dubyak GR, Humphreys BD, Sinkins WG. Maitotoxin and P2Z/$P2X_7$ purinergic receptor stimulation activate a common cytolytic pore. Am J Physiol 1999;277:C766–76.
[22] Murgia M, Pizzo P, Steinberg TH, Di Virgilio F. Characterization of the cytotoxic effect of extracellular ATP in J774 mouse macrophages. Biochem J 1992;288:897–901.
[23] Zanovello P, Bronte V, Rosato A, Pizzo P, Di Virgilio F. Responses of mouse lymphocytes to extracellular ATP. II. Extracellular ATP causes cell type-dependent lysis and DNA fragmentation. J Immunol 1990;145:1545–50.
[24] Ferrari D, Los M, Bauer MK, Vandenabeele P, Wesselborg S, Schulze-Osthoff K. P2Z purinoreceptor ligation induces activation of caspases with distinct roles in apoptotic and necrotic alterations of cell death. FEBS Lett 1999;447:71–5.
[25] Schulse-Lohoff E, Zanner S, Ogilvie A, Sterzel RB. Extracellular ATP stimulates proliferation of cultured mesangial cells *via* $P_2$-purinergic receptors. Am J Physiol 1992;263:F374–83.
[26] Harada H, Chan CM, Loesch A, Unwin RJ, Burnstock G. Induction of proliferation and apoptotic cell death *via* P2Y and P2X receptors, respectively, in rat glomerular mesangial cells. Kidney Int 2000;57:949–58.
[27] Buerstedde JM, Takeda S. Increased ratio of targeted to random integration after transfection of chicken B cell lines. Cell 1991;67:179–88.
[28] Kubista H, Hawkins TE, Patel DR, Haigler HT, Moss SE. Annexin-5 mediates a peroxide-induced $Ca^{2+}$ influx in B cells. Curr Biol 1999;9:1403–6.
[29] Dunn PM, Benton DC, Campos RJ, Ganellin CR, Jenkinson DH. Discrimination between subtypes of apamin-sensitive $Ca^{2+}$-activated $K^+$ channels by gallamine and a novel bis-quaternary quinolinium cyclophane, UCL 1530. Br J Pharmacol 1996;117:35–42.
[30] Hamill OP, Marty A, Neher E, Sakmann B, Sigworth FJ. Improved patch-clamp techniques for high-resolution current recording from cells and cell-free membrane patches. Pflugers Arch 1981;391:85–100.
[31] Koopman G, Reutelingsperger CP, Kuijten GA, Keehnen RM, Pals ST, van Oers MH. Annexin-V for flow cytometric detection of phosphatidylserine expression on B cells undergoing apoptosis. Blood 1994;84:1415–20.
[32] Murgia M, Hanau S, Pizzo P, Rippa M, Di Virgilio F. Oxidised ATP. An irreversible inhibitor of the macrophage purinergic P2Z receptor. J Biol Chem 1993;268:8199–203.
[33] Thompson EB. Special topic: apoptosis. Annu Rev Physiol 1998;60:525–32.
[34] Fadok VA, Voelker DR, Campbell PA, Cohen JJ, Bratton DL, Henson PM. Exposure of phosphatidylserine on the surface of apoptotic lymphocytes triggers specific recognition and removal by macrophages. J Immunol 1992;148:2207–16.
[35] Baricordi OR, Melchiorri L, Adinolfi E, Falzoni S, Chiozzi P, Buell G, Di Virgilio F. Increased proliferation rate of lymphoid cells transfected with the $P2X_7$ ATP receptor. J Biol Chem 1999;274:33206–8.
[36] Chiozzi P, Murgia M, Falzoni S, Ferrari D, Di Virgilio F. Role of the purinergic P2Z receptor in spontaneous cell death in J774 macrophage cultures. Biochem Biophys Res Commun 1996;218:176–81.
[37] Ferrari D, Chiozzi P, Falzoni S, Dal Susino M, Collo G, Buell G, Di Virgilio F. ATP-mediated cytotoxicity in microglial cells. Neuropharmacology 1997;36:1295–301.
[38] Coutinho-Silva R, Persechini PM, Bisaggio RD, Perfettini JL, Neto AC, Kanellopoulos JM, Motta-Ly I, Dautry-Varsat A, Ojcius DM. P2Z/$P2X_7$ receptor-dependent apoptosis of dendritic cells. Am J Physiol 1999;276:C1139–47.
[39] Bianchi BR, Lynch KJ, Touma E, Niforatos W, Burgard EC, Alexander KM, Park HS, Yu H, Metzger R, Kowaluk E, Jarvis MF, van Biessen T. Pharmacological characterization of recombinant human and rat P2X receptor subtypes. Eur J Pharmacol 1999;376:127–38.
[40] Nuttle LC, Dubyak GR. Differential activation of cation channels and non-selective pores by macrophage P2Z purinergic receptors expressed in Xenopus oocytes. J Biol Chem 1994;269:13988–96.
[41] Ding J, Takano T, Gao S, Han W, Noda C, Yanagi S, Yamamura H. Syk is required for the activation of Akt survival pathway in B cells exposed to oxidative stress. J Biol Chem 2000;275:30873–7.
[42] Pogue SL, Kurosaki T, Bolen J, Herbst R. B cell antigen receptor-induced activation of Akt promotes B cell survival and is dependent on Syk kinase. J Immunol 2000;165:1300–6.
[43] Salvesen GS, Dixit VM. Caspases: intracellular signaling by proteolysis. Cell 1997;91:443–6.
[44] Zoetewij JP, van de Water B, de Bont HJ, Nagelkerke JF. The role of a purinergic P2Z receptor in calcium-dependent cell killing of isolated rat hepatocytes by extracellular adenosine triphosphate. Hepatology 1996;23:858–65.
[45] Hawkins TE, Das D, Young B, Moss SE. DT40 cells lacking the $Ca^{2+}$-binding protein annexin-5 are resistant to $Ca^{2+}$-dependent apoptosis. Proc Natl Acad Sci USA 2002;99:8054–9.